ELSEVIER

Journal of Nuclear Materials 240 (1997) 100–111

journal of nuclear materials

Surface layers on a borosilicate nuclear waste glass corroded in $MgCl_2$ solution

Abdesselam Abdelouas [a,b,c,*], Jean-Louis Crovisier [b], Werner Lutze [d], Bernd Grambow [a], Jean-Claude Dran [e], Regina Müller [a]

[a] Forschungszentrum Karlsruhe, INE, Postfach 3640, 76021 Karlsruhe, Germany
[b] Centre de Géochimie de la Surface (CNRS), 1, rue Blessig, 67084 Strasbourg cedex, France
[c] University of New Mexico, Center for Radioactive Waste Management, SE-Suite 201, 1001 University Blvd., Albuquerque, NM 87106, USA
[d] University of New Mexico, 151 Farris Engineering Center, Albuquerque, NM 87131, USA
[e] CSNSM (IN2P3)-CNRS, 91405 Orsay, France

Received 2 July 1996; accepted 20 September 1996

Abstract

Surface layers on the French borosilicate nuclear waste glass, R7T7, corroded in $MgCl_2$ solution were studied to determine the composition, structure and stability of crystalline phases. The characteristics of the phases constituting the surface layer varied with the parameter $S/V \times t$, the glass surface area (S) to solution volume (V) ratio, times time (t). At low $S/V \times t$ values (< 360 days/m; ≤ 36 d) the surface layer was thin and contained mainly iron hydroxide particles and hydrotalcite crystals. At an intermediate $S/V \times t$ value (2800 d/m; 5.5 y) the surface layer contained hydrotalcite-, chlorite- and saponite-type phases. At the highest $S/V \times t$ value (10^7 d/m; 463 d) the major phases were saponite, powellite, barite and cerianite solid solutions. About 95% of the uranium and $> 98\%$ of the neodymium released from the glass were precipitated in the surface layer. In the 463 day experiment, 86% of the neodymium in the surface layer was in solid solution with powellite, the rest with saponite. Uranium was contained exclusively in saponite. High S/V ratios, typical of disposal conditions for vitrified high-level radioactive waste, favor retention of actinides in fairly insoluble corrosion products. Observation of similar corrosion products on natural glasses as on nuclear waste glasses lend support to the hypothesis that the host phases for actinides observed in the laboratory are stable over geological periods of time.

1. Introduction

In France, liquid high-level radioactive waste arising from commercial reprocessing of spent reactor fuel is converted into a glass known as R7T7. Non-radioactive specimens of this glass have been produced at the Commissariat à l'Energie Atomique laboratories in Marcoule, France (Table 1). These specimens have been studied extensively in Europe, mainly in France and in countries who have reprocessing contracts with the French and receive their high-level waste in the form of R7T7 glass for intermediate storage and eventual disposal in geological formations.

This study is a continuation of work started in the 1980s in Germany where a salt formation has been selected for the construction of a repository for radioactive waste [1]. Potential interactions of the glass with salt solutions under site specific conditions have been studied to provide data for repository safety analyses. In the beginning, the focus was on the corrosion kinetics of the glass rather than on surface layers and corrosion products. Work on this topic can be found in the literature [2–4]. Studies of surface layers were conducted to identify secondary phases in which fission products and actinides

* Corresponding author. University of New Mexico, Center for Radioactive Waste Management, SE-Suite 201, 1001 University Blvd., Albuquerque NM 87106, USA. Tel.: +1-505 272 7271; fax: +1-505 272 7304; e-mail: badria@unm.edu.

PII S0022-3115(96)00672-1

Table 1
Composition of R7T7 nuclear waste glass (in wt%)

SiO_2	45.48	ZrO_2	2.65
Al_2O_3	4.91	CoO	0.12
B_2O_3	14.02	Ag_2O	0.03
Na_2O	9.86	CdO	0.03
CaO	4.04	SnO_2	0.02
Fe_2O_3	2.91	Sb_2O_3	0.01
Cr_2O_3	0.51	TeO_2	0.23
P_2O_5	0.28	Cs_2O	1.42
Li_2O	1.98	BaO	0.60
ZnO	2.50	La_2O_3	0.90
NiO	0.74	Ce_2O_3	0.93
SrO	0.33	Pr_2O_3	0.44
Y_2O_3	0.20	Nd_2O_3	1.59
MoO_3	1.70	UO_2	0.52
MnO_2	0.72	ThO_2	0.33

would be retained after release from the glass [5,6]. However, a major fraction of the surface layers was not characterized, consisting presumably of clay minerals and amorphous material. Samples from these investigations are used in this work to characterize the clay minerals and to study phase formation, transformation, chemical reactions between phases, retention of waste constituents and long-term phase stability.

Recent experiments with highly radioactive R7T7 glass also prepared by CEA show that there are no differences in the time and temperature dependence (110–190°C) between the corrosion of the radioactive and a non-radioactive glass [7]. This suggests that the corrosion mechanism is not affected by radiation. Leachate acidification results from the formation of glass corrosion products, in particular from the clay mineral saponite. No additional effect from radiation was noticed. This suggests that the same kinds of solid corrosion products are formed, independent of radiation. The concentrations of actinide elements and technetium in the leachate indicated that only minor fractions of these elements were retained in the solid glass corrosion products.

2. Experimental

This section summarizes the experimental conditions under which the corrosion of the non-radioactive borosilicate glass R7T7 was studied by Lutze et al. [2,3] leading to the surface layers investigated in this work.

2.1. Materials and methods

Samples of the French borosilicate nuclear waste glass, R7T7, were produced at the Commissariat à l'Energie Atomique laboratories in Marcoule, France. Oxides and carbonates were mixed and then melted at 1200°C [8]. The glass composition is given in Table 1. The glass contains a mixture of inactive waste constituents closely simulating the composition of the French high-level liquid waste arising from their commercial fuel reprocessing plants at La Hague. There are 11.25 wt% fission product oxides, 3.83 wt% corrosion product oxides and 0.85 wt% actinide oxides (U and Th) in the glass. MnO_2 was added to account for RuO_2 and TcO_2, CoO for RhO_2 and NiO for PdO. Pm_2O_3, Sm_2O_3, Eu_2O_3 and Gd_2O_3 are contained in the weight fraction of La_2O_3. ThO_2 was added to simulate NpO_2, PuO_2, AmO_2 and CmO_2.

Corrosion tests were performed applying glass surface area (S) to solution volume (V) ratios between $1.4\ m^{-1} < S/V < 21\,700\ m^{-1}$. Duration of the experiments varied from 0.25 day to 2006 days. The temperatures were 190°C and 200°C, as indicated in Table 2. To realize S/V ratios of $1.4\ m^{-1}$ and $10\ m^{-1}$, glass coupons, $10 \times 10 \times 2$ mm, were used. To attain an S/V ratio of $21\,700\ m^{-1}$, glass powder was used ranging in size from 200 μm to 230 μm yielding an average grain size of about 240 μm. The volume of the leachant was about 20 ml. The powder was washed in water and acetone until all fines were removed. A glass coupon was added to the powder to facilitate samples preparation for surface layer characterization after corrosion. The corrosion experiments were executed in Teflon™-lined autoclaves after introducing the glass samples and the salt solution. The leachant is a reference solution (Table 3) for corrosion experiments with borosilicate nuclear waste glass in Germany. The composition is that of the hexary Na^+, K^+, Mg^{2+}, Cl^-, SO_4^{2-}, H_2O system at the point Q, i.e., a solution in equilibrium with halite, sylvite, kainite and carnallite. Solid NaCl was added to the brine at room temperature to maintain halite saturation at 190° and 200°C. After reaction, the glass was rinsed with deionized water at 80°C until salt residues were

Table 2
Corrosion conditions of glass samples and analytical techniques used to study surfaces

Time (days)	Temperature (°C)	Volume (cm^3)	S/V (m^{-1})	Techniques [a]
0.25	190	27	10	SEM, STEM
2	190	29	10	SEM, STEM
3	190	29	10	SEM, STEM
12	190	61	10	SEM, STEM
36	190	55	10	SEM, STEM
113	190	15	21,700	SEM, STEM, XRD
463	190	25	21,700	SEM, STEM, XRD
2006	200	200	1.4	SEM, STEM, XRD, RBS

[a] SEM, STEM: scanning and transmission electron microscopy; XRD: X-ray diffraction; RBS: Rutherford backscattering spectrometry.

Table 3
Chemical composition of salt solution (mol/kg of water) [8]

Na	0.378
K	0.967
Mg	4.471
Cl	9.933
SO_4	0.177
Ionic strength	14.9
pH_{corr}	6.6

pH_{corr}: corrected for liquid junction potential.

removed. Further details of the experimental procedure are given in Ref. [2].

2.2. Analyses of leachates

After cooling, aliquots of leachates were taken immediately, passed through a 450 nm filter and diluted by a factor of 10 to enable chemical analysis by inductively coupled plasma atomic emission spectrometry (ICP-AES). The solutions were analyzed for Si, B, Sr, Ca, Zn, Li, Zr, Cr, Fe, Al, Mn, Ni, Nd and Ce [2]. pH measurements were carried out in the undiluted solutions at room temperature and corrected for the liquid junction potential, according to a procedure described by Grambow and Müller [9].

2.3. Analyses of solid corrosion products

Surface layers on the corroded glass were investigated in this study using a Jeol JSM 840 scanning electron microscope (SEM) equipped with a TRACOR TN 5500 energy-dispersive X-ray spectrometer (EDX). Ultra-thin sections (50–80 nm thick) for STEM analyses were prepared with an ultramicrotome equipped with a diamond knife and using a procedure by Ehret et al. [10] to obtain micrometer-sized specimens. With these samples corrosion phases were observed at high resolution [11–15]. The ultrathin sections were examined by lattice fringe imaging, selected area diffraction, microdiffraction and semi-quantitative thin-film X-ray microanalysis using a Philips CM 12 transmission electron microscope. The X-ray microanalyses were obtained using an EDAX PV 9900 spectrometer. Relative errors of the analytical results were estimated to be about $\pm 10\%$.

Surface layers from samples corroded for 113, 463 and 2006 days were examined by X-ray powder diffraction recorded on a Philips 1120/90 X-ray diffractometer with Ni-filtered CuKα radiation. In addition, diffractograms were taken from oriented specimens of the corrosion products on the 2006 day sample. One spectrum was taken from an as-prepared oriented specimen. Subsequent spectra were taken from specimens saturated with ethylene glycol or hydrazine at room temperature and after heating at 490°C for 4 h to identify clay minerals by their 00l basal reflections. Spectra were recorded between $2° < 2\theta < 30°$.

The glass adjacent to the surface layer on the 2006 day sample was analyzed by Rutherford backscattering spectrometry (RBS). The experiment was conducted after mechanical removal of the surface layer. Details of RBS are given in Ref. [16].

3. Results

3.1. Leachate analyses

Results of leachate and pH analyses are given in Table 4. The progress of corrosion is expressed in units of grams of corroded glass per cubic meter of leachant, as measured

Table 4
Results of solution analyses (normalized concentration in g/m^3)

	S/V (m^{-1}). Time (days)							
	10					1.4	21 700	
	0.25	2	3	12	36	2006	113	463
B	**35**	**121**	**132**	**174**	**254**	**1417**	**55 748**	**108 797**
Si	27.9	110.2	124.6	173.1	228.7	103.3	210.5	238.7
Li	n.m.	n.m.	n.m.	154.2	288.8	1522.4	47 740.0	79 530.5
Mn	70.2	190.9	131.7	43.9	61.4	522.3	22 785.0	69 006.0
Zn	n.m.	n.m.	n.m.	104.1	267.7	1483.9	31 573.5	54 684.0
Sr	n.d.	100.3	103.9	186.3	236.4	1429.1	8029.0	14 864.5
Mo	n.d.	90.0	110.3	123.5	211.8	1385.3	759.5	434.6
U	n.d.	n.d.	n.d.	n.d.	n.d.	n.d.	n.d.	2604.0
Nd	n.d.	n.d.	n.d.	n.d.	n.d.	872.7	868.0	1519.0
La	n.d.	n.d.	n.d.	n.d.	n.d.	1050.8	n.d.	1844.5
pH	n.m.	n.m.	n.m.	6.53	6.55	6.29	4.66	4.22

Concentrations of boron in solution are assumed to be a measure of the amount of *dissolved glass*.
n.d.: not detected; n.m.: not measured.

by each of the elements listed. It is assumed that the concentration of boron in solution is a correct measure of the amount of glass corroded. This assumption is not always justified [17] but in this case it is a good approximation. Table 4 shows that all concentrations increase with time, except for molybdenum. Mo concentrations increase at low and decrease at high S/V ratios with time. pH values decrease from an initial 6.4 ± 0.1 to 4.2 ± 0.1 at $S/V = 21\,700\ m^{-1}$ after 463 days. A decrease in pH is typical of glass corrosion experiments in Mg-rich solutions and is due to the formation of saponite [9]. In the work by Grambow and Müller [9], the existence of saponite was derived from thermodynamic considerations. This work provides experimental evidence for the presence of a saponite-type clay mineral.

3.2. Solid corrosion products; low S / V

3.2.1. SEM, XRD, RBS and STEM results

SEM/EDX analyses of glass samples corroded for short periods of time (0.25 to 36 days) at low S/V ratios (Table 5) show hexagonal crystals, Fig. 1a. These crystals are rich in Mg, Al and Cl. The phase is a variant of hydrotalcite $[Mg_6Al_2CO_3(OH)_{16} \cdot 4H_2O]$ and was first identified by Abdelouas et al. [18,19] when the glass R7T7 was corroded in a concentrated $MgCl_2$–$CaCl_2$ solution.

After 2006 days, the surface of the glass was covered by layers (Fig. 1(b)). The layers are exfoliated as a result of drying and are composed of the following major elements: Si, Al, Mg, Zr, Cr and Cl. There are also small bright spheres scattered throughout the layers, about 2 μm in size, composed of ZrO_2 (53%), ThO_2 (6%), SiO_2 (30%), Al_2O_3 (3%), Nd_2O_3 (5%) and MgO (3%), i.e. wt%. This material may be a variant of zircon ($ZrSiO_4$). There was not enough material to determine the structure by X-ray diffraction. TEM samples for electron diffraction could not be prepared because the white spheres could not be separated from the matrix to the extent necessary to identify zircon unambiguously. However, there is striking similarity between the chemical composition of this material and a zircon observed in a pegmatite by Hasewaga [20]. The weight ratio of Si/Zr is 0.30 in pure zircon. In the bright spheres in the surface layer, this ratio is 0.35, close to that of a zircon (0.31) formed in the Oklo natural nuclear reactor in Gabon, Africa and close to that of a zircon (0.34) formed in the lava of the exploded nuclear reactor at Chernobyl, Ukraine [21].

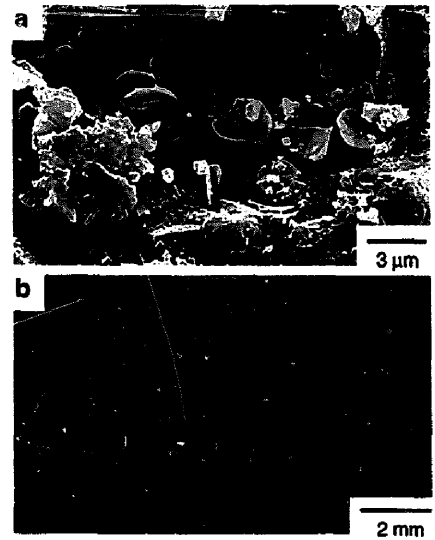

Fig. 1. (a) SEM photograph of hydrotalcite formed on the 2 day sample. (b) SEM photograph of the 2006 day sample showing the exfoliated surface layer.

The layered material on the sample of the 2006 day experiment consists of saponite, chlorite and hydrotalcite. Phase identification was accomplished by X-ray diffraction of oriented samples after introduction of organic molecules

Table 5
Secondary phases formed during the corrosion (XRD and SEM-TEM/EDX results)

	S/V (m^{-1}), Time (days)							
	10					1.4	21 700	
	0.25	2	3	12	36	2006	113	463
Hydrotalcite (Mg, Al, Cl)	+	+	+	+	+	+	–	–
Chlorite (Mg, Al, Fe, Si)	–	–	–	–	–	+	–	–
α-FeOOH	–	–	–	–	+	–	–	–
Zircon (Th, Nd, Zr)SiO_4	–	–	–	–	–	+	–	–
Saponite (Mg, Al, Fe, Si, Mo, Zr, U, Nd)	–	–	–	–	–	+	+	+
Barite (Sr, Ba)SO_4	–	–	–	–	–	–	+	+
Powellite (Nd, Pr, La, Ca, Na)MoO_4	–	–	–	–	–	–	+	+
Cerianite (CeO_2)	–	–	–	–	–	–	+	+

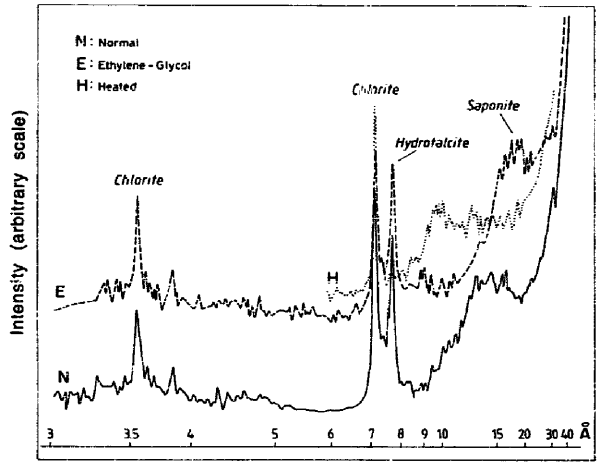

Fig. 2. X-ray diffractogram pattern of oriented clays (chlorite, hydrotalcite and saponite; 2006 day sample).

into the crystal structures. Fig. 2 shows reflections typical of saponite. The 001 plane d spacing increased from 1.5 to 1.85 nm after saturation with ethylene glycol and decreased to 1.0 nm after heating to 490°C. There are also reflections from chlorite for which there is no detectable change of the 001 and 002 plane d spacing after any treatment with organic molecules. The presence of hydrotalcite is indicated by the disappearance of the reflection of the 003 plane at 0.77 nm after heating to above 300°C, due to decomposition [22]. As expected, hydrazine treatment caused no change in the diffraction pattern of hydrotalcite.

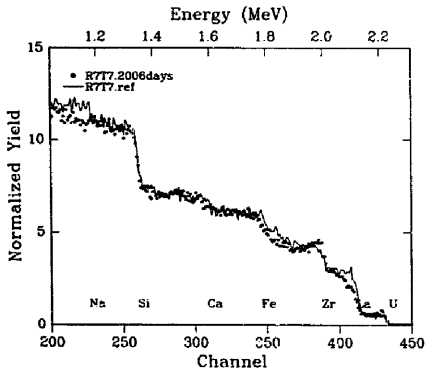

Fig. 3. RBS spectra of pristine (R7T7 ref) and corroded glass (R7T7 2006 days).

The results of an RBS experiment with the 2006 day glass sample are shown in Fig. 3. The persistence of the Si edge and its similarity to that of the pristine glass indicates that the glass phase is not heavily altered. Na, Fe and REE are depleted in the 5.0 nm thick glass layer assessable to backscattering. Zr and probably U are slightly enriched. As discussed by Petit et al. [23], this enrichment is probably not a result of phase formation such as oxy-hydroxides or hydroxides. However, the change in glass composition, i.e., the substitution of several elements for H_3O^+, may explain the change in the intensity of the backscattering signal. A relative enrichment of Zr in the glass surface has also been observed by several authors [13,14,24,25] on R7T7 glass samples corroded under various experimental conditions in aqueous solutions.

An effort was made to detect Mg by RBS in the glass beneath the surface layer but none was found. This suggests that Mg-rich silicates such as saponite are formed exclusively within or on top of the surface layer after release of SiO_2 from the glass. These findings do not support finding by Berger et al. [26] and Guy et al. [27]. These authors studied the alteration of basaltic glass in seawater and explained the formation of Mg-rich silicates by diffusion of Mg into the leached glass and subsequent reaction with Si and Al.

STEM analyses of the glass samples corroded for short periods of time (< 36 days) did not show any crystalline phases in the surface layers. The 36 day sample contains poorly crystallized Fe-rich particles with a microdiffraction pattern compatible with α-FeOOH (0.201, 0.157 and 0.115 nm). The glass sample corroded for 2006 days contains chlorite, hydrotalcite and saponite. The chemical composi-

Table 6
Electron diffraction data for 10 saponite crystals from the corroded glass samples: data in nm

113 day sample					463 day sample				
1.087	1.038	0.951	–	–	1.038	0.951	1.038	–	–
0.453	0.457	0.466	–	0.453	–	–	–	0.457	–
–	0.448	0.448	0.448	–	0.439	0.442	0.446	–	0.441
0.313	0.322	0.308	0.351	–	0.308	0.326	0.305	–	0.340
0.259	0.256	0.256	0.256	0.254	–	–	–	0.262	–
0.248	–	–	–	–	–	0.242	0.248	–	0.248
0.152	0.151	–	0.155	0.151	–	0.149	0.148	0.151	0.148
0.130	–	–	0.131	0.130	–	–	0.128	–	–

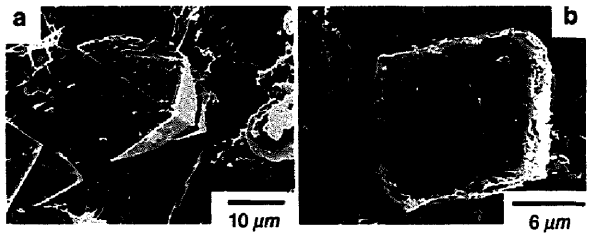

Fig. 4. SEM photograph of powellite (a) and barite (b) in the surface layer after 463 days of glass corrosion.

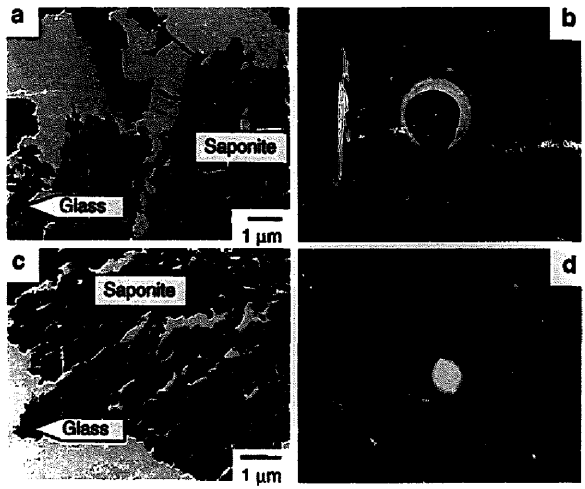

Fig. 5. (a) Ultramicrotomic thin section of the glass/surface layer interface (113 day experience). (b) Electron diffraction of a saponite crystal in the surface layer. (c) Ultramicrotomic thin section of the glass/surface layer interface (463 days). (d) Electron diffraction pattern showing the 001 reflections of saponite (463 days).

Table 7
Chemical composition of saponite

	113 days	463 days	2006 days
MgO	20.6±1.8	23.5±1.4	21.4±2.7
Al_2O_3	7.2±1.3	7.8±1.9	9.1±2.3
SiO_2	60.5±3.4	60.4±2.7	58.3±3.5
CaO	0.6±0.4	0.3±0.3	0.9±0.7
Cs_2O	0.5±0.5	0.2±0.3	0.4±0.4
Nd_2O_3	0.9±0.5	0.3±0.4	1.6±0.9
Fe_2O_3	3.9±0.5	3.8±0.6	2.6±1.1
NiO	1.1±0.4	1.1±0.3	0.7±0.3
ZnO	0.3±0.3	0.3±0.2	–
UO_2	1.7±1.3	0.9±0.7	1.6±1.1
ZrO_2	1.5±0.8	0.6±0.3	1.9±1.0
MoO_3	1.2±0.4	0.8±0.4	1.5±0.6
N.A.	10	10	6

N.A.: Number of analyses.

tion of the saponite identified in this sample is given in Table 7.

3.3. Solid corrosion products; high S / V

3.3.1. SEM, XRD and STEM results

SEM/EDX analyses conducted by Rother et al. [5] of surface layers of R7T7 glass samples corroded in concentrated salt solutions at 190°C and at high S/V ratios showed three phases (solid solutions of waste constituents with powellite, barite and cerianite) in addition to those identified in this work on samples corroded at low S/V ratios. No experiments were conducted by Rother et al. [5] to identify the clay minerals in the surface layers. Powellite ($CaMoO_4$) shown in Fig. 4(a) and barite shown in Fig. 4(b) were analyzed for the purposes of this work. Powellite was rich in Nd_2O_3 (23), Pr_2O_3 (6), and La_2O_3 (3) in wt%; barite contained 6 to 8% SrO by weight. The composition of these minerals did not change significantly between 113 and 463 days.

Saponite was identified in the present study by X-ray diffraction using the 0.457, 0.207, 0.171 and 0.153 nm d spacing. All phases identified in the surface layers from experiments at low and high S/V ratios are listed in Table 5. Fig. 5(a) shows an ultramicrotome thin section of the glass sample corroded for 113 days (Table 4). A 5 μm thick corrosion layer and pristine glass are visible. Electron microdiffraction experiments were conducted with five samples selected from the corrosion layer to identify the clay minerals. The results are summarized in Table 6. Fig. 5(b) shows a diffraction pattern typical of the smectite in the surface layer of the corroded glass. The average value of the basal d spacing is 1.025 nm which is typical of a smectite dehydrated under the electron beam. The average chemical composition obtained from the analyses of various samples is given in Table 7. Major constituents are Si, Mg, Al and Fe. Minor constituents are Zr, U, Nd and Mo. Electron diffraction and chemical analyses data are consistent with the structure and composition of known saponite-type clay minerals [28].

Fig. 5(c) shows an ultramicrotome thin section of the glass sample corroded for 463 days. A 21 μm thick corrosion layer and pristine glass are visible. Electron microdiffraction experiments were conducted with five samples selected from the corrosion layer to identify the clay minerals. The results are summarized in Table 6. Fig. 5(d) shows a diffraction pattern typical of the basal plane 001 of smectite in the surface layer of the corroded glass. The average value of the basal d spacing is 1.01 nm which is typical of a smectite dehydrated under the electron beam. The values for the 001 d spacing obtained from the 113 day and the 463 day experiment are the same, considering the scattering of the values in Table 6. An average chemical composition is given in Table 7. There are only insignificant differences in the clay composition between this and the 113 day corrosion experiment concerning Si, Al and Fe. As for the 113 day experiment, electron diffraction and chemical analyses data are consistent with the structure and composition of known saponite-type clay minerals.

4. Discussion

4.1. The role of Mg

The effect of Mg on the composition of a surface layer becomes evident when comparing the layers of glass samples corroded in Mg-rich and in Mg-poor salt solutions. Results from corrosion experiments in Mg-poor salt solutions have been reported in a previous study [15]. High Mg concentrations lead to the formation of an almost entirely crystalline layer (Fig. 5(a), (c)). Amorphous silica and other constituents such as Al, precipitated on the glass surface, react with Mg and form a saponite-type clay mineral. The yield of this reaction is a function of the Mg inventory in the leachant. When the Mg supply is limited and exhausted before the corrosion experiment is terminated, the surface layer consists of a crystalline layer facing the solution as well as an amorphous part facing the glass, as observed by Abdelouas et al. [15]. These authors found, beneath a layer of saponite, a silica gel layer in which Zr, Nd and U were accumulated. Apparently, Mg diffuses from the solution into the amorphous precipitate on the glass surface where it forms saponite. This mechanism would explain why in the present study no Mg was detected in the underlying glass phase.

4.2. Retention of waste constituents in surface layers

During glass corrosion, waste constituents (Table 1) participate in the formation of crystalline corrosion prod-

Table 8
Retention of oxides in the corrosion layer of the glass calculated in percent of oxides contained in the glass before corrosion

	Time (days)							
	0.25	2	3	12	36	2006	113	463
SiO_2	20	9	5	1	10	93	99.6	99.8
MnO_2		0	6	75	77	66	62	42
SrO		17	21	0	7	8	87	88
MoO_3		26	17	29	17	11	97.2	99.1
Nd_2O_3						44	98.5	98.6
La_2O_3						32		98.5
UO_2								95

ucts on the glass surface and become part of their structures. Calculated fractions of retained waste constituents are listed in Table 8 together with the fraction of retained SiO_2. Fig. 6 shows a plot of the data from Table 8 as a function of the amount of dissolved glass (values from Table 4). The curves show that retention is low when the concentration of dissolved glass is low. Retention is much higher at high concentrations of dissolved glass (463 day experiment, Table 8), particularly for Mo, Nd, La and U. For these elements retention values range between 95 and over 99%. Sr is retained to about 90%. Only Mn seems to increase and then decrease with increasing glass dissolution.

Mn was added to simulate Tc, one of the longest lived and therefore most important constituent of high-level radioactive waste. In light of the significant differences in the chemistry of Mn and Tc, it is questionable whether the observed retention pattern for Mn represents that of Tc. Studies with Tc have shown that a significant fraction of Tc is present in the form of TcO_2 which was detected as

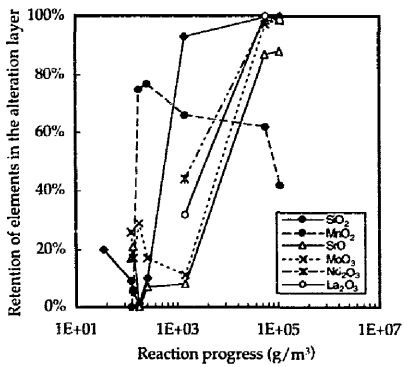

Fig. 6. Retention of oxides in the corrosion layer of the glass calculated in percent of oxides contained in the glass before corrosion.

an insoluble precipitate in the glass phase [29]. Using square wave voltammetry, Freude et al. [29] detected also some Tc in its heptavalent state, even at 1200°C. In contrast, higher valence states of Mn (Mn^{4+} to Mn^{7+}) are unstable at high temperatures. Mn occurs in its lower valence states, preferably Mn^{2+} and a little bit of Mn^{3+}. Mn is readily soluble in the glass phase [30]. Tc is sparingly soluble.

The waste constituents Mo, Nd and La are major components of powellite, a potential host phase for Am and Cm. If the results obtained for Nd and La can be applied to Am and Cm, the dissolved fraction of these actinides in solution will be small (< 1%, Table 8).

The 2006 day experiment conducted at $S/V = 1.4\ m^{-1}$ ($S/V \times t = 2{,}800$ d/m) yields much lower concentrations of glass constituents in solution than the 463 day experiment at $S/V = 21\,700\ m^{-1}$ ($S/V = 10^7$ d/m). Therefore, phases like powellite and barite have not yet formed. Waste constituents listed in Table 8 are partially retained in saponite and other phases of the surface layer.

Saponite and powellite are the most abundant corrosion products. In the 113 and 463 day samples almost all of the silica released from the glass has been transformed into saponite. Mo is contained in saponite and in powellite. The quantity of SiO_2 in saponite is: SiO_2(saponite) = SiO_2(total) − SiO_2(leachate). The quantities of Fe, Al, Mo, Nd, U, Ni and Zr in saponite were calculated using the STEM data in Table 7. The Nd content of powellite, for example, is: Nd(powellite) = Nd(total) − Nd(leachate) − Nd(saponite). The results of the calculations are given in Table 9. Except for U and Zr, there is fair agreement between the total amount of each element released from the glass and the sum of the fractions calculated from independent measurements. For uranium the discrepancy may just be an experimental error, since more U was found in saponite than was leached from the glass. Only a fraction of total Zr released from the glass was found in saponite. The remainder is suspected to be contained in zircon, as in the case of the 2006 day experiment. It was not possible to separate the phases in the surface layer to

Table 9
Distribution of selected elements among solution, saponite and powellite (mg)

	113 days				463 days			
	total	sol.	sap.	pow.	total	sol.	sap.	pow.
SiO_2	380	1.4	378.6	–	1237	2.8	1234.2	–
Fe_2O_3	24	–	24.4	–	79.1	–	77.6	–
Al_2O_3	41	–	45.1	–	133.5	–	159.4	–
MoO_3	14.2	0.4	7.5	6.3	46.2	0.4	16.3	29.5
Nd_2O_3	13.3	0.2	5.6	7.5	43.2	0.6	6.1	36.5
UO_2	4.3	–	10.6	–	14.1	0.7	18.4	–
NiO	6.2	–	6.9	–	20.1	0.9	22.5	–
ZrO_2	22.1	–	9.4	–	71.5	–	12.3	–

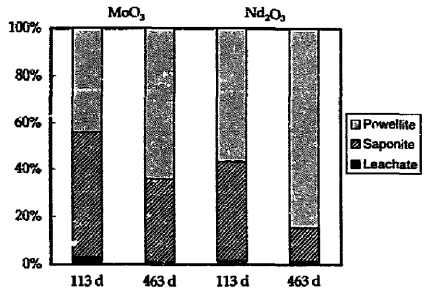

Fig. 7. Distribution of Mo and Nd among secondary phases and the leachate for the 113 and 463 day samples.

the extent necessary to find zircon. The table shows that Fe, Al and Ni are contained only in saponite. The balance of Fe yields the best results and is consistent with the wide use of Fe in geochemical materials balance calculations [31–33]. Table 9 shows that, after 113 days, 56.5% of Nd_2O_3 released from the glass is contained in powellite, 42% in saponite and 1.5% in solution. With increasing reaction progress more Mo is released from the glass and more powellite forms. This leads to a depletion of Mo in saponite in favor of powellite. After 463 days, there are 84.6% of Nd_2O_3 in powellite and only 14% in saponite, but the content in solution did not change. The calculated distribution of Mo and Nd among the secondary phases and the leachate is illustrated in Fig. 7 for the 113 day and 463 day experiments.

4.3. Stability of individual phases

The first crystalline phase to form on the glass surface is a hydrotalcite-type compound. Its formation requires Al to be released from the glass to exceed hydrotalcite's solubility product. As Al and Si are released at an atomic ratio of 1:14, clay minerals should begin to form while more hydrotalcite is crystallizing. This can be concluded when comparing the analytical data for Si at low and high S/V values in Table 4. Glass dissolution data calculated from silica concentrations in the leachate indicate that an apparent Si saturation is reached between 12 and 36 days. The Si concentration is the same as in the 113 and 463 day experiments at the high S/V ratio, whose leachates are expected to be silica saturated. Slow precipitation kinetics may explain why chlorite and saponite are observed after 2006 days but not after 36 days.

Although the atomic ratio of Fe and Si in the glass is only 1:35, the solubility of FeOOH at pH 6.6 is low enough for iron precipitates to form in the surface layer. After longer corrosion periods Fe precipitates are no longer seen in the surface layers. As iron is not in solution, it is concluded that it has been incorporated in clay minerals.

After 36 days, 6.7 mg/l ZrO_2 have been released from the glass, certainly enough to detect zircon under the transmission electron microscope, if not under the scanning electron microscope. Slow reaction kinetics may explain why zircon is not found after 36 days but is found after 2006 days.

As discussed above, there is enough silica after 36 days to form saponite. The initial consumption of Al in hydrotalcite may explain why the appearance of saponite is delayed. In saponite the charge deficit, resulting from partial substitution of Si by Al in the tetrahedral layer, is compensated by cations in the interlayers. The dominating element in the interlayer is Mg from solution but waste elements (Table 1) can substitute for Mg. This is evidenced by the composition of the surface layer after 2006 days: 11% of MoO_3, 32% of Nd_2O_3 and 44% of La_2O_3 released from the glass are contained in the layer. The remaining fractions of these elements are in solution (Table 4).

Table 5 shows that the solid phases on the samples corroded at high S/V ratios are different from those on samples corroded at low S/V ratios. Saponite is the only phase found at both low (after 2006 days) and high S/V ratios. The nature of the retention of waste constituents in the surface layer is a function of the parameter $S/V \times t$. Surface layers on samples corroded at the highest experimentally achievable S/V and for the longest times t will certainly yield the most realistic data concerning long-term phase stability and composition. While an S/V on the order of 20,000 m^{-1} as applied in this work is close to what can be realized, a defensible compromise must be reached concerning the duration of an experiment. As the product $S/V \times t$ is directly proportional to the concentration of *dissolved glass* in the leachant, and silica saturation was reached at $S/V \times t \leq 3.6 \times 10^2$ d/m, an $S/V \times t = 10^7$ d/m with $t > 1$ year was considered sufficient to provide long-term saturation for silica and enough time for nucleation and slow crystal growth. It is our working hypothesis that the phases observed on the 463 day sample (Table 5) are not subject to structural transformation. To test and verify the hypothesis, the phases will be compared with those observed on natural glasses corroded over geological time periods (next chapter). Changes in the chemical composition within the phases may continue to some extent, if the experiment were continued beyond 463 days. However, the extent of compositional changes is expected to be less significant than that observed between 113 and 463 days for two reasons: firstly, the disequilibria between some phases, e.g., saponite/powellite, diminish with time; secondly, the appearance of additional phases that would significantly affect the existing ones is unlikely, because most of the major glass constituents (> 1 wt% in the glass) are already involved in phase formation. Only borate has not yet formed any phases but will eventually. The effect of S/V on the glass corrosion has also been investigated for diluted solutions [34–37].

For example, Mazer et al. [37] studied the SRL 131 borosilicate glass corrosion in deionized water at 90°C as a

function of S/V ratio at constant $S/V \times t$. The main conclusion was that glasses reacted at different S/V ratios results in different surface layers, even though the quantity of dissolved glass is the same. Since certain phases were observed at the low S/V ratio but not at the high ratio, it was concluded that precipitation kinetics are responsible for different surface layer compositions. This conclusion agrees with ours concerning saponite and zircon.

The phases composing the surface layer on the 463 day and on the 113 day samples are saponite, powellite, barite and cerianite. Iron hydroxide, hydrotalcite and chlorite are no longer present. These phases are obviously intermediate reaction products and are transformed into more stable phases. At the high S/V ratio of 21 700 m^{-1}, rapid enrichment of rare earth elements takes place in the leachate and the rare earths become increasingly soluble with decreasing pH. The final pH was 4.22 in the 463 day experiment (Table 4). Simultaneously, the rare earth elements are incorporated into saponite and two new rare earth phases precipitate, a powellite- and a cerianite-type mineral. The chemical composition, for example, of the powellite solid solution is fairly constant. There is only a 3 mol% change in the REE content between 113 and 463 days (REE = rare earth elements). Barite ($BaSO_4$) formed a solid solution with Sr. The Sr content in the $(Ba,Sr)SO_4$ increased from 5.9 mol% by about 31% to 7.7 mol% between 113 and 463 days. The chemical composition of saponite, with respect to some waste constituents, decreased drastically between 113 and 463 days while its Mg content increased. Saponite lost 33% of MoO_3, 47% of UO_2 and 60% of ZrO_2 and Nd_2O_3, respectively. This loss was compensated by a gain in Mg, indicating that at least fractions of these elements are accommodated in the interlayer of the saponite structure. The fractions of the major elements, Si, Al and Fe, in saponite, remained practically constant with time. The concentration of the minor constituent Ni remained also constant with time, indicating its strong bondage in the octahedral site, together with Al and Fe.

The loss of Mo, Nd, U and Zr from saponite between 113 days and 463 days (Table 7) can be explained by consumption of these elements during growth of the powellite and cerianite-type phases. Powellite and cerianite are already present on the 113 day sample. Neither phase is seen in the experiments at low S/V. Their formation may require a high degree of supersaturation prior to nucleation and the growth rate is expected to be slow. The substitution of Mo, Nd, U and Zr for Mg is governed by ion-exchange. As ion-exchange is a solid state diffusion process, it is not clear whether this process or crystal growth limits the extraction of these elements from saponite.

4.4. Secondary phases on the borosilicate glass and on natural glasses

Secondary phases (palagonites) on basaltic glasses, naturally altered in seawater, are described as a mixture of phyllosilicates [27,31,32,38] often associated with zeolites and calcite. Zeolites and calcite are not found in the surface layers of R7T7 glass because these phases are not stable at the low pH of the leachates (Table 4). The occurrence of hydrotalcite in palagonite was described by Ramanaidou and Noack [39] in samples from the axial rift of the Red Sea. These authors suppose that hydrotalcite is the precursor of the phyllosilicates, e.g., saponite, found in palagonites.

The sequence of appearance of the phases in the R7T7 glass surface layer, hydrotalcite and Fe-hydroxides initially, then replacement by saponite, is the same as that observed by Crovisier et al. [40–42], Thomassin [43] and Thomassin et al. [44,45] for basaltic glass altered in seawater in the laboratory. Thomassin et al. [44] conducted corrosion experiments with basaltic glass. They showed that the earliest stage of alteration is characterized by the formation of a leached layer on the pristine glass followed by precipitation of Fe-hydroxides in the layer and then crystallization of hydrotalcite. They also showed that hydrotalcite transforms into Al-serpentine or chlorite, two closely related minerals and then into a Mg-rich smectite, due to the increase of silica concentration in solution. Crovisier et al. [32,42] calculated the equilibrium constant of hydrotalcite and showed, using the geochemical code DISSOL [46,47], that hydrotalcite is thermodynamically not stable in seawater and is replaced by saponite. Again, these results are in good agreement with what was observed for the R7T7 borosilicate nuclear waste glass.

Saponite is one of the phyllosilicate-type phases found on volcanic glasses altered in fresh water and in seawater [27,31,40]. Powellite and barite are corrosion products typical of vitrified high-level waste, because of their high Ba and Mo content, compared with natural glasses whose Ba and Mo contents are low. However, powellite has been observed as an alteration product of rhyolitic glass, naturally altered in salt brines in the Zagros salt domes in Iran [48]. Barite is a relatively abundant mineral and forms preferentially in salt formations and hydrothermal systems (e.g., Ref. [49]). Solid solutions of Sr and Ba in barite have been observed by several authors [15,50–53]. Cerianite is found in weathered rocks (phonolite, syenite, tuff) and is one of the most stable secondary phases, rich in rare earth elements [54–56]. Fletcher [56] described an assemblage of barite, cerianite and other secondary phases in a weathered volcanic environment in Bolivia. These findings, altogether, support the hypothesis that the corrosion products formed on R7T7 waste glass are stable over geological periods of time and that they are the final products of the corrosion process.

Abdelouas [53] studied the alteration of rhyolitic glass in lacustrine core sediments from a drill hole in the salar of Uyuni in Bolivia. Erosion processes have deposited rhyolitic glass in the salar from surrounding volcanic rock. The sediments consist mainly of evaporate phases and detritals and are saturated with NaCl solution [57]. Hence,

the glass shards were exposed to a saturated salt solution for geological periods of time. The samples investigated are about 10 to 30000 years old. Although there were no surface layers attached to the glass, its corrosion products were found and identified in the sediments as Mg-rich smectite, Sr-rich barite, celestite ($SrSO_4$), cerianite, pyrite (FeS_2) and alunite ($KAl_3(SO_4)_2(OH)_6$). The Sr content (7 wt%) of the Bolivian barite is close to that of barite precipitated on the R7T7 glass.

5. Conclusions

1. Studies of surface layers on glasses corroded at low values of $S/V \times t$ (glass surface area (S), solution volume (V) and time (t)) yield information on the early stages of the process, e.g., the nature of transient phases such as hydrotalcite, Fe-hydroxides and chlorite.
2. Studies of surface layers on glasses corroded at high values of $S/V \times t$, on the order of 10^7 d/m, yield information on phases that are stable after the initial phases have disappeared.
3. The chemical composition of the phases observed at high $S/V \times t$ values may continue to change to some extent, if longer a duration of the corrosion experiments were selected than here. However, the type of phases is likely to remain unchanged. This hypothesis is supported by studies of secondary phases on volcanic glasses altered in nature over geological periods of time. Hence, information on long-term stable corrosion products of nuclear waste glasses can be obtained from experiments in the laboratory.
4. Thorough analysis of the chemical composition of the corrosion products provides data on the retention of hazardous (radioactive) constituents after release from the glass.
5. The duration of corrosion experiments at high S/V ratios must be long enough for phase nucleation and transformation to take place. Also, enough glass must be corroded to involve as many glass constituents as possible in the formation of secondary phases, leaving only minor constituents (Ag, Cd, Sn, etc., Table 1) and the most soluble ones, such as boron and lithium in solution.
6. The type of phases observed on different glasses vary with glass composition and with the initial composition of the leachant. For example, nuclear waste glasses contain enough Ba to form barite if sulfate is in solution. Concentrated Mg salt solutions are acidic at high $S/V \times t$. As a result, zeolites, abundant secondary phases on altered natural glasses, cannot form.

Acknowledgements

The authors wish to thank P. Karcher for SEM pictures, G. Morvan and G. Ehret for the preparation of ultrathin sections and J.L. Cesar, R. Wendling and P. Larqué for the X-ray diffraction experiments.

References

[1] W. Lutze, K.D. Closs, G. Tittel, P. Brennecke and W. Kunz, in: Proc. Int. Conf. Nuclear Waste Management and Environmental Remediation, Booki No. 10354A, eds. D. Alexandre, R. Baker, R. Kohout and J. Marek (The American Society of Mechanical Engineers, 1993) p. 79.
[2] W. Lutze, R. Müller and W. Montserrat, Mater. Res. Soc. Symp. Proc. 112 (1988) 575.
[3] W. Lutze, R. Müller and W. Montserrat, Mater. Res. Soc. Symp. Proc. 127 (1989) 81.
[4] B. Grambow, W. Lutze and R. Müller, Mater. Res. Soc. Symp. Proc. 257 (1992) 143.
[5] A. Rother, W. Lutze and P. Schubert-Bischoff, Mater. Res. Soc. Symp. Proc. 257 (1992) 57.
[6] W. Lutze and B. Grambow, Radiochim. Acta 58&59 (1992) 3.
[7] B. Grambow, A. Loida, L. Kahl and W. Lutze, Mater. Res. Soc. Symp. Proc. 353 (1989) 39.
[8] F. Pacaud, A. Jacquet-Francillon, A. Terki and S. Fillet, Mater. Res. Soc. Symp. Proc. 127 (1989) 105.
[9] B. Grambow and R. Müller, Mater. Res. Soc. Symp. Proc. 176 (1990) 229.
[10] G. Ehret, J.L. Crovisier and J.P. Eberhart, J. Non-Cryst. Solids 86 (1986) 72.
[11] J.L. Crovisier and J.P. Eberhart, J. Microsc. Spectrosc. Electron. 10 (1985) 171.
[12] T.A. Abrajano, J.K. Bates, A.B. Woodland, J.P. Bradley and W.L. Bourcier, Clays Clay Miner. 38 (1990) 537.
[13] J.L. Crovisier, E. Vernaz, J.L. Dussossoy and J. Caurel, Appl. Clay Sci. 7 (1992) 47.
[14] A. Abdelouas, J.L. Crovisier, J. Caurel and E. Vernaz, C.R. Acad. Sci. Paris 317 (Série II) (1993a) 1333.
[15] A. Abdelouas, J.L. Crovisier, W. Lutze, R. Müller and W. Bernotat, Eur. J. Miner. 5 (1995) 526.
[16] W.K. Chu, G.W. Mayer and M.A. Nicolet, Backscattering Spectrometry (Academic Press, New York, 1984).
[17] E. Vernaz and A. Lodding, Workshop on In situ Testing of Radioactive Waste Forms and Engineered Barriers, Oct. 13–16, Corsendonk, Belgium (1992), in press.
[18] A. Abdelouas, J.L. Crovisier, W. Lutze and W. Bernotat, C.R. Acad. Sci. Paris 317 (Série II) (1993b) 1067.
[19] A. Abdelouas, J.L. Crovisier, W. Lutze, B. Fritz, A. Mosser and R. Müller, Clays Clay Miner. 5 (1994) 526.
[20] S. Hasegawa, Sci. Rep. Tohoku Univ. Ser. 3: 5 (1957).
[21] V. Sere., J. Carpena and J.R. Kienast, 15e Réunion des Sciences de la Terre, Nancy, 26–28 Apr. (1994) T18.
[22] G.W. Brindley and S. Kikkawa, Clays Clay Miner. 28 (1980) 87.
[23] J.C. Petit, G. Della-Mea, J.C. Dran, M.C. Magonthier, P.A. Mando and A. Paccagnella, Geochim. Cosmochim. Acta 54 (1990) 1941.
[24] J. Caurel, E. Vernaz and D. Beaufort, Mater. Res. Soc. Symp. Proc. 176 (1990) 306.
[25] Z. Andriambololona, N. Godon and E. Vernaz, Appl. Geochem. (Suppl. 1) (1992) 23.

[26] G. Berger J. Schott and M. Loubet, Earth Planet. Sci. Lett. 25 (1987) 385.
[27] C. Guy, J. Schott, C. Destrigneville and R. Chiappini, Geochim. Cosmochim. Acta 56 (1992) 4169.
[28] S. Caillère, S. Henin and M. Rautureau, Minéralogie des Argiles. Classification et Nomenclature (Masson, Paris, 1982).
[29] E. Freude, W. Lutze, C. Rüssel and H.A. Schaeffer, Mater. Res. Soc. Symp. Proc. 127 (1989) 199.
[30] M.B. Volf, Chemical Approach to Glass (Elsevier, 1984).
[31] J. Honnorez, Publ. Vulkaninstitut Immanuel Friedlaender, Vol. 9 (Birkhaüser Verlag, Basel, 1972).
[32] J.L. Crovisier, J. Honnorez and J.P. Eberhart, Geochim. Cosmochim. Acta 51 (1987) 2977.
[33] V. Daux, J.L. Crovisier, C. Hemond and J.C. Petit, Geochim. Cosmochim. Acta 58 (1994) 4941.
[34] E.C. Ethridge, D.E. Clark and L.L. Hench, Phys. Chem. Glasses 20 (2) (1979) 35.
[35] C.Q. Buckwalter, L.R. Pederson and G.L. McVay, J. Non-Cryst. Solids 49 (1982) 397.
[36] K. Lemmens and P. Van Iseghem, Mater. Res. Soc. Symp. Proc. 257 (1992) 49.
[37] J.J. Mazer, J.K. Bates, B.M. Biwer and C.R. Bradley, Mater. Res. Soc. Symp. Proc. 257 (1992) 73.
[38] P. Dudoignon, A. Meunier, D. Beaufort, A. Gachon and D. Buiges, Chem. Geol. 76 (1989) 385.
[39] E. Ramanaidou and Y. Noack, Mineral. Mag. 51 (1987) 139.
[40] J.L. Crovisier, J.P. Eberhart, J.H. Thomassin, T. Juteau, J.C. Touray and G. Ehret, C.R. Acad. Sci. Paris 294 (Série II) (1982) 989.
[41] J.L. Crovisier, J.H. Thomassin, T. Juteau, J.P. Eberhart, J.C. Touray and P. Baillif, Geochim. Cosmochim. Acta 47 (1983) 377.
[42] J.L. Crovisier, B. Fritz, B. Grambow and J.P. Eberhart, Mater. Res. Soc. Symp. Proc. 50 (1985) 273.
[43] J.H. Thomassin, PhD thesis, Université d'Orléans (1984).
[44] J.H. Thomassin, J.L. Crovisier, J.C. Touray, T. Juteau and F. Boutonnat, Bull. Soc. Géol. (France) 1 (1985) 217.
[45] J.H. Thomassin, F. Boutonnat, J.C. Touray and P. Baillif, Eur. J. Mineral. 1 (1989) 261.
[46] B. Fritz, Sci. Géol. Mém., Univ. Louis Pasteur, Strasbourg 41 (1975).
[47] B. Fritz, Sci. Géol. Mém., Univ. Louis Pasteur, Strasbourg 65 (1981).
[48] P. Sulovsky, in: Proc. 8th Meeting of European Union of Geosciences, Terra Abstr., Vol. 1 (Strasbourg, 1995) p. 202.
[49] N. Shikazono, Geochim. Cosmochim. Acta 58 (1994) 2203.
[50] E. Brower and J. Renault, N. M. Bur. Mines Miner. Resour. Circ. 116 (1971) 21.
[51] J. Denis and G. Michard, Bull. Mineral. 106 (1983) 309.
[52] C. Monnin and C. Galinier, Chem. Geol. 71 (1988) 283.
[53] A. Abdelouas, PhD Thesis, Université Louis Pasteur, Strasbourg (1996).
[54] A.R. Graham, Am. Miner. 40 (1955) 560.
[55] C. Frondel and U.B. Marvin, Am. Miner. 44 (1959) 882.
[56] C.J.N. Fletcher, J. Geol. Soc. (London) 139 (1982) 664.
[57] F. Risacher and B. Fritz, Chem. Geol. 90 (1991) 211.